2015-01-01

Modeling Of The Response Of A Memcapacitor For An Impulse, Step, Ramp, And Sinusiodal Inputs

Ghassan Khalil Kachmar
University of Texas at El Paso, gkachmar@utep.edu

MODELING OF THE RESPONSE OF A MEMCAPACITOR

FOR AN IMPULSE, STEP, RAMP, AND SINUSIODAL INPUTS

GHASSAN KHALI L KACHMAR

Department of Electrical and Computer Engineering

APPROVED:

Joseph H. Pierluissi, Ph.D., Chair

Behzad Djafari-Rouhani, Ph.D.

José Mireles García , Ph.D.

Charles Ambler, Ph.D.
Dean of the Graduate School

Dedication

To my parents,
my wife, Lourdes, and
my Children, Yasmin, Jonathan and Aaliyah

MODELING OF THE RESPONSE OF A MEMCAPACITOR FOR IMPULSE, STEP, RAMP AND SINUSOIDAL INPUTS

By

GHASSAN KHALIL KACHMAR, MSEE

DISSERTATION

Presented to the Faculty of the Graduate School of

The University of Texas at El Paso

in Partial Fulfillment

of the Requirements

for the Degree of

DOCTOR OF PHILOSOPHY

Department of Electrical and Computer Engineering

THE UNIVERSITY OF TEXAS AT EL PASO

December 2014

Acknowledgements

I would like to thank my advisor and committee chair Dr. Joseph H. Pierluissi for his immense support, guidance, patience, and encouragement throughout my Ph.D. program. I also like to thank my other committee members Dr. Jose Mireles and Dr. Behzad Djafari-Rouhani for their valuable time and support.

Special thanks for Jesus Gutierrez for his help and ideas. I also like to thank Dr. David Zubia and Dr. Sergio Loya for their support and guidance.

Abstract

Micro-Electro-Mechanical Systems, or MEMS, is a technology of very small scale devices. The dimensions of MEMS can vary from below one micron to several millimeters. MEMS have some mechanical functionalities such as the moving plate of a parallel plate capacitor (memcapacitor). MEMS researchers and developers have demonstrated an extremely large number of microsensors for almost every possible sensing modality including temperature, pressure, inertial forces, and chemical species. The equation of motion of the moving plate of a memcapacitor is governed by a non-linear differential equation with no known exact solution. Most research into determining the theoretical response of a memcapacitor to a time varying voltage, was done for the steady-state case. Non-linearity of the displacement of the plate in a memcapacitor presents a challenge in determining the plate's position and capacitive detection.

This dissertation presents an exact closed form solution to the non-linear differential equation for an impulse input, and an approximate analytical closed form solution without the steady state assumption for step, ramp, and sinusoidal sources. The analytical method is based on solving the non-linear differential equation by linearizing the inverse- quadratic electro-static force in the equation and approximating it with the linear terms of its power series expansion. A comparison between the analytical and numerical (MATLAB) simulation shows that the displacement of the electrode can be described with an accurate closed form approximation. The analytical results follow closely within 1% of the numerical results for small signals, thus allowing control of the plate's position and capacitive detection with reasonable accuracy.

Table of Contents

List of Figures

Chapter 1: Introduction and Background

Microelectromechanical systems (MEMS) are systems with electrical and mechanical components that are scaled down to the micrometer scale Figure 1.1. It is an interdisciplinary field, which borrows its microfabrication techniques from the integrated circuit industry. Apart from the fabrication techniques from the integrated circuit industry, many micromachining techniques that are specific to MEMS have been developed. The development of microfabrication techniques and the realization of MEMS role in demanding environments have led to the development of complex MEMS structures. Some of the commercially successful MEMS applications are accelerometers, microsensors (e.g. inertial sensors, pressure sensors, magnetometers, and chemical sensors), microactuators (e.g. micromirrors, microrelays, microvalves) and ink-jet printer heads [1].

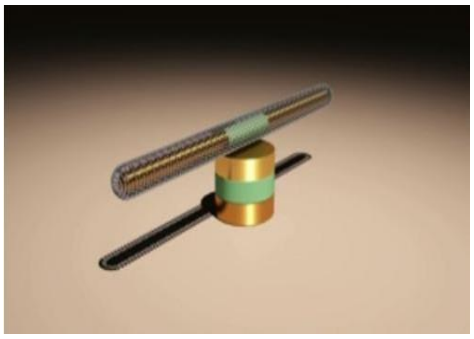

Figure 1.1: Picture of the world smallest motor [1].

In 1964, a team from Westinghouse led by Harvey Nathanson produced the first batch fabricated MEMS device. This device joined a mechanical component with electronic elements and was called a resonant gate transistor (RGT). Shown in Figure 1.2, the RGT was a gold resonating MOS gate structure. It was approximately one millimeter long and it responded to a very narrow range of electrical input signals. It served as a frequency filter for integrated circuits by transmitting only those signals within the designed range to an output circuit while ignoring all other frequencies [2].

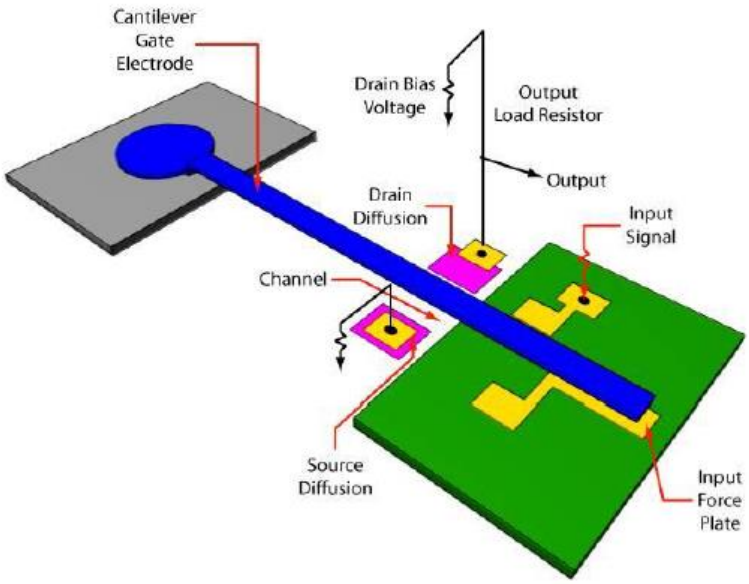

Figure 1.2: Resonant Gate Transistor [2].

In 1979, Hewlett Packard came up with an alternative to dot matrix printing called Thermal Inkjet Technology (TIJ). This printing technique rapidly heats ink, creating a tiny bubble. When the bubble pops, the ink droplet squirts through a nozzle; an array of these nozzles are part of the complete inkjet print head and allows the rapid creation of an image onto paper and other media. Silicon micromachining technology is used to manufacture the nozzles. The nozzles are made very small and are densely packed for high resolution printing. Since HP first came up with the TIJ,

improvements have been made to make the nozzles smaller and more densely packed to improve resolution. Many printers available today use the thermal ink jet technology [2].

In 1999 Lucent Technologies developed the first MEMS optical network switch. Optical switches are optoelectric devices, consisting of a light source and a detector that produces a switched output. It provides a switching function in a data communications network [2].

MEMS have been developed in the past decades, especially in the last fifteen years. In the beginning of 1990s, MEMS emerged with the aid of the development of integrated circuit (IC) fabrication processes, in which sensors, actuators, and control functions are fabricated in silicon. Since then, remarkable research progresses have been achieved in MEMS under the strong capital promotions from both government and industries. In addition to the commercialization of some less integrated MEMS devices, such as microaccelerometers, inkjet printer head, micromirrors for projection, the concepts and feasibility of more complex MEMS devices have been proposed and demonstrated for the applications in such varied fields as microfluidics, aerospace, biomedical, chemical analysis, wireless communications, data storage, display, and optics [1].

Scientists are still discovering new ways to combine MEMS sensors and actuators with emerging bioMEMS technology. Applications include drug delivery systems, insulin pumps, DNA arrays, lab-on-a-chip (LOC), glucometers, neural probe arrays, and microfluidics, just to name a few. The area of bioMEMS has only just begun to be explored. Research and development at this time is occurring at a very rapid pace [2].

MEMS applications involve energy transformation in which input energy of one form is converted to output energy of a different form. A transducer can be defined as a device that accepts energy from one system and supplies it usually in another form to a second system. Sensors and actuators are devices that transduce energy from one form into another. Sensors sense nonelectrical

parameters and convert them into electrical signals, while actuators sense electrical signals and convert them to mechanical motion.

Electrostatic actuators are used in many micro-electro-mechanical systems due to their simplicity of operation and ease of fabrication see Figure 1.3. Electrostatic actuation works on the principle of attraction between oppositely charged objects. These actuators generally have smaller area for capacitive surfaces due to geometry limitations and hence generate small force and displacement. The motion of the actuators takes place close to the substrate and hence it is difficult to use these kinds of actuators to create actuation far from the substrate [3]. Parallel plate actuators (memcapacitors) generate a force directly proportional to the product of the charges on the plates and inversely proportional to the square of the distance between them, hence the small displacement. Large displacements can lead to pull-in instability in which the two plates collide with each other.

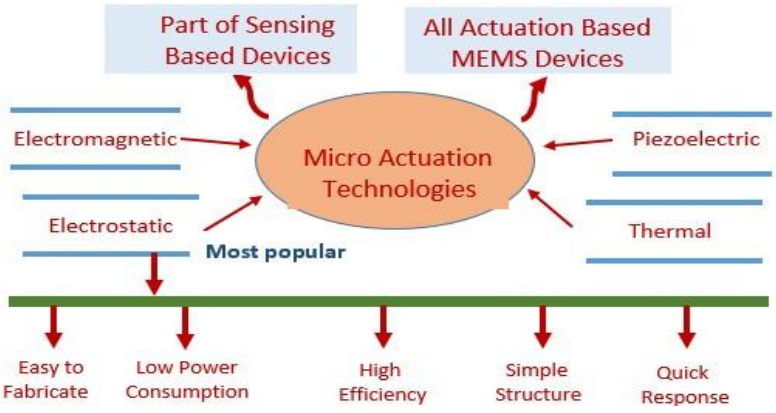

Figure 1.3: Types of actuators [4].

There is a wide variety of MEMS devices that are produced for commercial use and to be used for a variety of applications. Figure 1.4 shows the emerging MEMS forecast. It shows the current and the forecast market of MEMS.

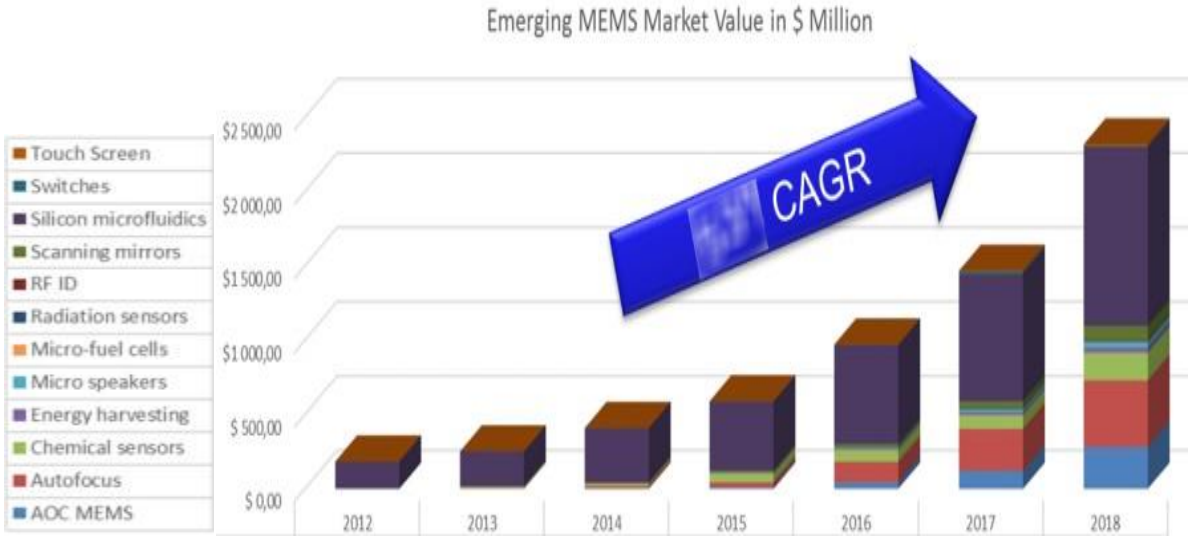

Figure 1.4: The current and emerging
MEMS market forecast [5].

Chapter 2 discusses the behavior of the parallel plate capacitor and shows the various equations used to analyze the behavior of a parallel plate actuator. Also, the derivation of the differential equation that governs the behavior of the memcapacitor for any input source.

Chapter 2: MEM Devices Operation

2.1 Introduction

This chapter discusses the basic operation of parallel-plate capacitors and memcapacitrors. The first section of this chapter presents the basic operation of a parallel-plate capacitor and the relations between its various parameters. Also, it discusses the operation of a memcapacitor and the non-linear relationship between the force acting on the plates and the distance separating them. The second section presents the dynamic model of the system and the derivation of the characteristic differential equation (2.9) that governs it.

2.2 Basic Operation of a Non-Fringing Capacitive MEM

Capacitors are constructed by separating two sheets of conductors, usually metallic based, by a thin layer of insulating material. In a parallel-plate capacitor, the sheets are flat and parallel as shown in Figure 2.1. The insulator material between the plates, called a dielectric, can be, air, mylar, polyester, polypropylene, mica, or a variety of other materials [6].

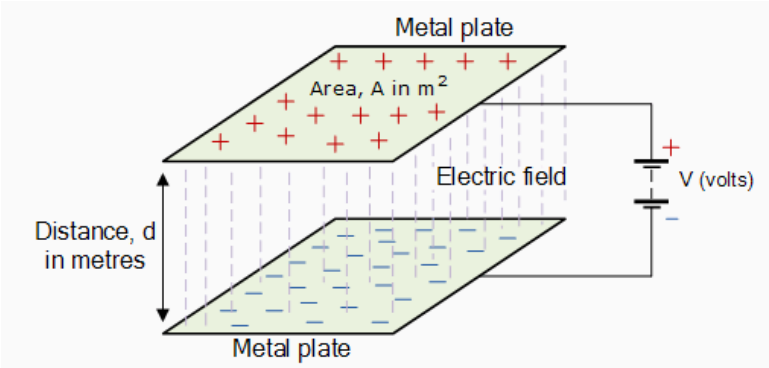

Figure 2.1: A parallel-plate capacitor [7].

As current flow through the capacitor, charge accumulates on the plates. In an ideal capacitor, the stored charge Q is proportional to the voltage between the plates [5].

$$Q = CV \tag{2.1}$$

The constant of proportionality is the capacitance C,

where
$$C = \frac{A\varepsilon_0}{d} \tag{2.2}$$

The current I is the time rate of flow of charge, that is

$$I = \frac{dQ}{dt} \tag{2.3}$$

The electric field produced by each plate is

$$E = \frac{Q}{2A\varepsilon_0}$$

The force of attraction between the two plates, Figure 2.2, is equal to the electric field produced by one plate multiplied by the charge on the other:

$$F = Q\frac{Q}{2A\varepsilon_0} = \frac{(CV)^2}{2A\varepsilon_0} = \frac{A\varepsilon_0 V^2}{2d^2} \tag{2.4}$$

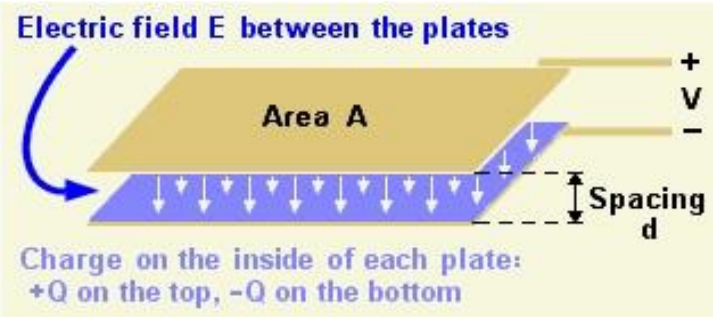

Figure 2.2: Forces between the plates
of a capacitor [8].

The force between the plates is inversely proportional to the square of the distance between them. Figure 2.3 shows the variation of the force with the plate's separation for different voltage sources.

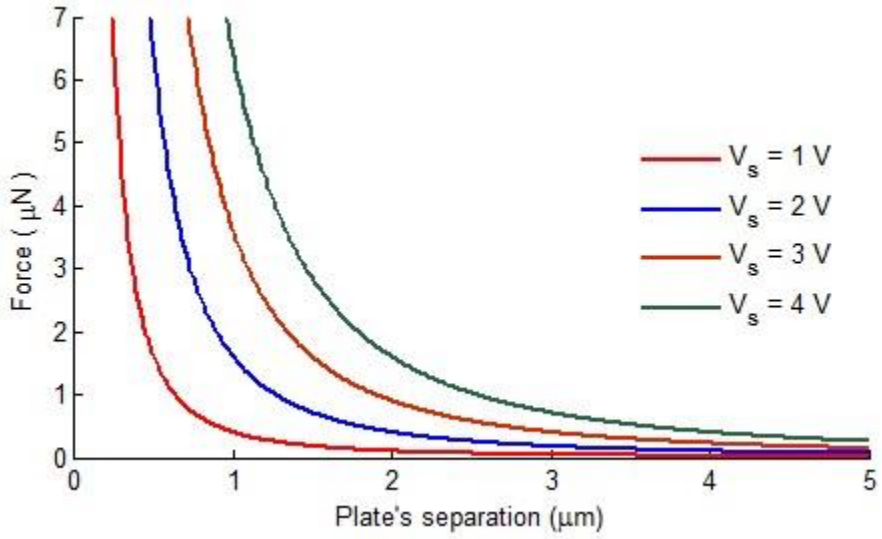

Figure 2.3: Variation of the force with the plate's separation for different voltage sources.

The force is maximum when the plates touch each other and minimum when the separation is at an original value of 5 μm.

Figure 2.4, shows the variation of the force between the plates with respect to the voltage source with a fixed separation of 5 μm.

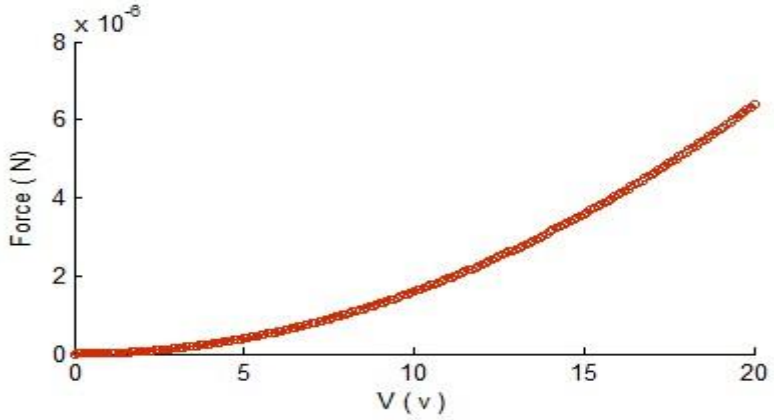

Figure 2.4: Variation of the force with the voltage.

Figure 2.5 shows the variation of the force between the plates with respect to the separation for various voltages.

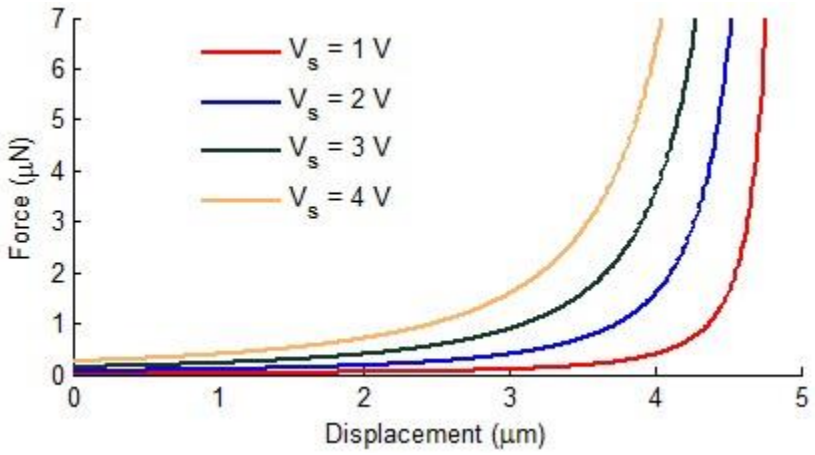

Figure 2.5: Variation of the force with the displacement for various voltages.

In the case of a memcapacitor, the force can be expressed as [6]:

$$F_e = \frac{A\varepsilon_0 V_s^2}{2(d - y(t))^2} \tag{2.5}$$

where

F_e is the electrostatic force between the plates

$y(t)$ is the displacement of the plate

t is time

A is the area of the plate

d is the separation between the plates

ε_0 is the permittivity of free space

V_s is the voltage source

Figure 2.6 shows the variation of the force between the plates with respect to their separation and potential.

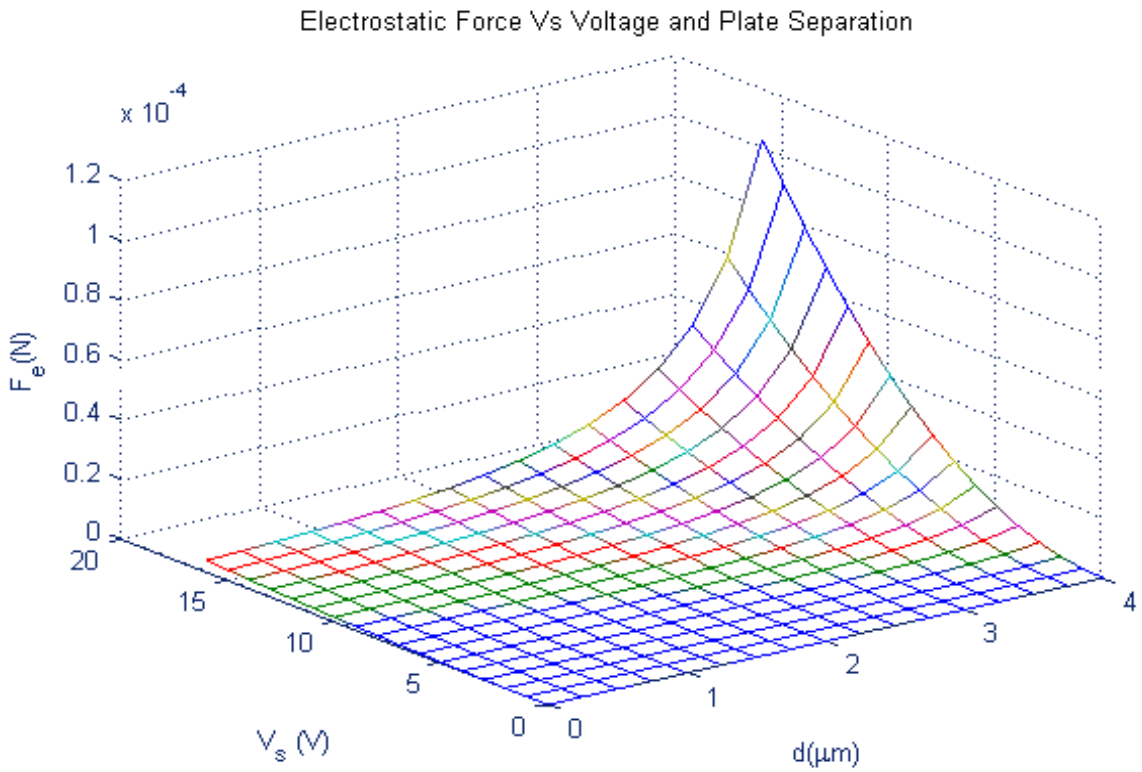

Figure 2.6: Variation of the force between the plates with respect to their separation and potential.

2.3 The Characteristic Differential Equation of a Non-Fringing Capacitive MEM

In the case of a memcapacitor, the upper plate is flexible and free to move in the vertical direction while the bottom plate is fixed as shown in Figure 2.7. When a voltage is applied across the plates, the electric force applied on the top electrode pulls it towards the bottom electrode, once the electrode is displaced, an elastic recovery force by the spring tends to pull the upper plate back towards its original position [11].

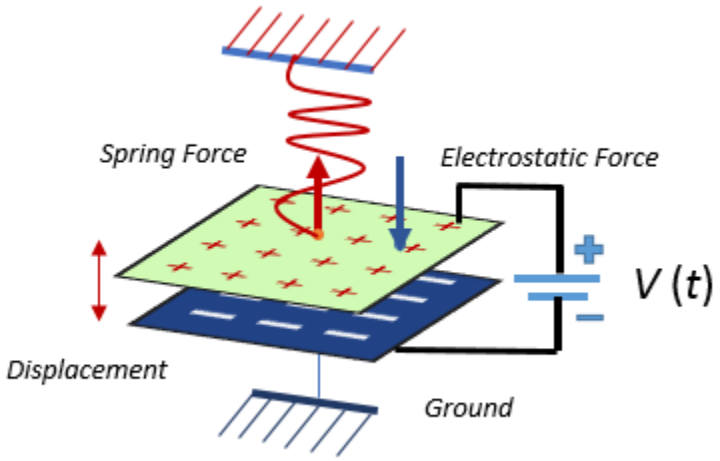

Figure 2.7: A MEMS diagram.

Let $y(t)$ be the displacement of the plate. The forces acting on the plate, shown in Figure 2.8 are:

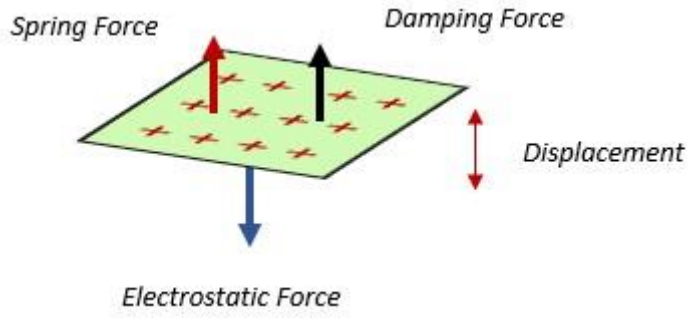

Figure 2.8: Free body diagram of a MEMS plate.

The damping force $$F_d = d_c \frac{dy(t)}{dt} \tag{2.6}$$

the spring force $$F_s = ky(t) \tag{2.7}$$

and the electrostatic force $$F_e = \frac{A\varepsilon_0 V_s^2}{2(d - y(t))^2} \tag{2.8}$$

Applying the first principle of dynamics

$$\sum F = ma$$

we get

$$m\frac{d^2y(t)}{dt^2} + d_c\frac{dy(t)}{dt} + ky(t) = \frac{A\varepsilon_0 V_s^2}{2\ (d - y(t))^2} \tag{2.9}$$

The system is non-linear due to the inverse variation of the electrostatic force with the square of the separation of the plates. There is no known solution to (2.9), solutions found by [9] and [10] are solutions for the steady state case. In the steady state case, assuming the inertial and viscous damping forces are small, see Figure 2.9, (2.9) simplifies to

$$ky(t) = \frac{A\varepsilon_0 V_s^2}{2(d - y(t))^2} \tag{2.10}$$

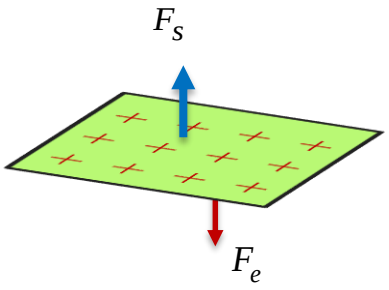

Figure 2.9: Forces applied on the upper plate
in the steady state case.

Equation (2.10) has three solutions. One solution has no physical meaning since $y > d$, one stable, and one unstable solution as shown Figure 2.10.

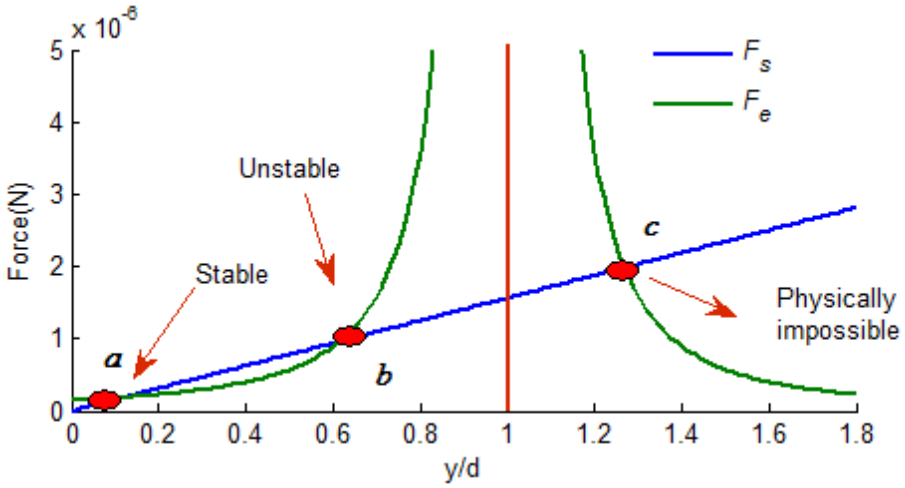

Figure 2.10: The dependence of the electrostatic and spring forces on displacement.

From Figure 2.10 we can see that the solution corresponding to point *b* is not a stable solution. If a small disturbance moves the mass back a little, the recovery force F_s will be larger than the electrostatic attractive force in quantity and move it back further until it falls to point *a*. On the other hand, if a disturbance moves the mass a little farther from point *b*, the electrostatic force will always be larger than the elastic recovery force and the mass will move forward continuously until falling into contact with the fixed electrode. However, the solution corresponding to point *a* is a stable one as the mass will always return to the balanced position after a disturbance force moving it away from the point [11].

Thus with

$$F\ \ y(t), V_s\ = \frac{A\varepsilon_0 V_s^{\ 2}}{2\ \ d - y(t)\ ^2} - ky(t) \tag{2.11}$$

then the balanced displacement is determined by

$$\frac{A\varepsilon_0 V_s^{\ 2}}{2(d - y(t))^2} - ky(t) = 0 \tag{2.12}$$

Even though a desired upper plate position can be attained with applying a certain voltage, it is important to examine methodically and in details its transient behavior and stability in order to understand its dynamics.

The Principle of Minimum Potential Energy: *Of all displacements satisfying the given boundary conditions of an elastic solid, those that satisfy the equilibrium equations make the potential energy a minimum* [12].

Let y_{eq} be an equilibrium state and let y_i an arbitrary direction. If the minimum potential energy $E_{potential}$ is at y_{eq}, then in a given neighborhood of y_{eq} , one has [13]:

If $y_{eq} > y_i$ then $E_{potential}\ (y_{eq}) < E_{potential}\ (y_i)$

If $y_{eq} < y_i$ then $E_{potential}\ (y_{eq}) < E_{potential}\ (y_i)$, thus

$$\left.\frac{\partial E_{potential}(y_{eq})}{\partial y_i}\right|_{y_i > y_{eq}} > 0$$
$$\left.\frac{\partial E_{potential}(y_{eq})}{\partial y_i}\right|_{y_i < y_{eq}} < 0 \tag{2.13}$$

Thus for stability, we must have $\frac{\partial E_{potential}(y)}{\partial y} = 0$ and $\frac{\partial^2 E_{potential}(y)}{\partial^2 y} > 0$ see Figure 2.11.

With $$E_{potential}(y) = \int_{y_{eq}}^{y} \left(ky - \frac{A\varepsilon_0 V_s^{\,2}}{2(d-y)^2} \right) dy = \frac{1}{2} ky^2 - \frac{A\varepsilon_0 V_s^{\,2}}{2(d-y)}$$

$$\frac{\delta E_{potential}(y)}{\delta y} = ky - \frac{A\varepsilon_0 V_s^{\,2}}{2(d-y(t))^2} = 0 \qquad (2.14)$$

and

$$\frac{\partial^2 E_{potential}(y)}{\partial^2 y} = k - \frac{A\varepsilon_0 V_s^{\,2}}{(d-y(t))^3} > 0 \qquad (2.15)$$

From (2.14) and (2.15) we get $y < \frac{d}{3}$.

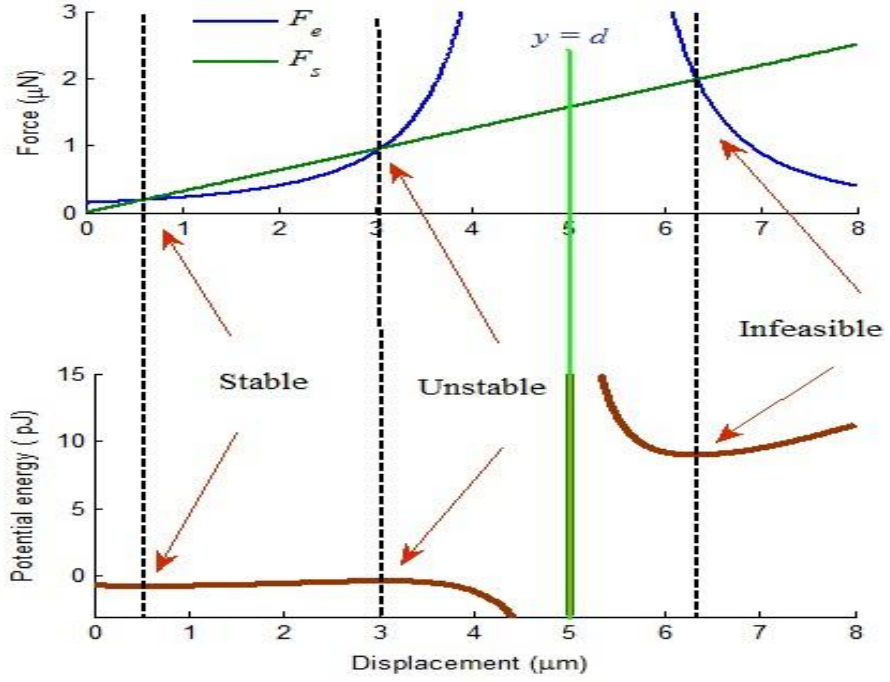

Figure 2.11: Forces acting on the plate and its potential energy.

This means stability is obtained when the displacement of the upper electrode is less than one third of its original distance from the fixed electrode.

For a specific mechanical structure, *k* is a constant. From Figures 2.12, 2.13, and 2.14 we can see that the curve for F_e moves up when increasing the input voltage V_s. Therefore, the points *a* and *b* move closer when increasing the value of V_s. It is conceivable that, for a critical voltage *Vpi*, points *a* and *b* merge. For any voltage larger than *Vpi*, there will be no intersection between the two curves, and the plates will collide. The phenomenon is known as the pull-in-effect [11].

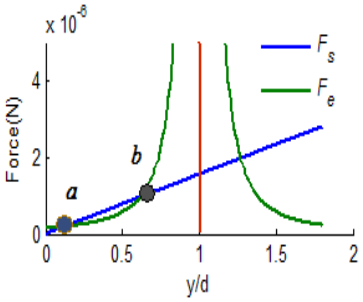

Figure 2.12: *Vs* < *Vpi*.

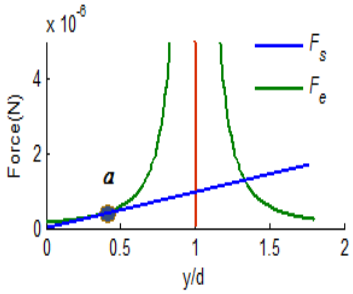

Figure 2.13: *Vs* = *Vpi*.

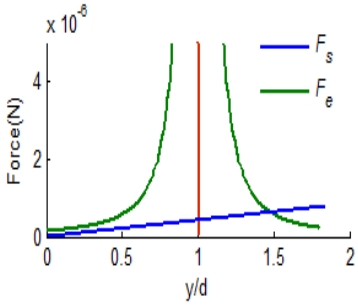

Figure 2.14: *Vs* > *Vpi*.

The pull-in-voltage can be found by solving (2.14) with $y = \frac{d}{3}$ yielding,

$$V_s = \sqrt{\frac{8kd^3}{27A\varepsilon_0}} \tag{2.16}$$

With parameters for the MEMS device provided by the Universidad Autonoma de Ciudad Juarez, MX, which are parameters used in a design using SUMMIT-V technology and considering a vacuum level of $1\text{x}10^{-5}$ Torr, namely,

$\varepsilon_0 = 8.854\text{x}10^{-12}$	F / m,	$d = 5\text{x}10^{-6}$	m
$k = 0.3125$	N / m,	$d_c = 10^{-4}$	Kg / s
$m = 2\text{x}10^{-6}$	Kg,	$A = 9\text{x}10^{-8}$	m^2

The pull-in-voltage is 3.811 volts. Any input voltage greater than 3.811, will drive the plates into contact as shown in Figure 2.15.

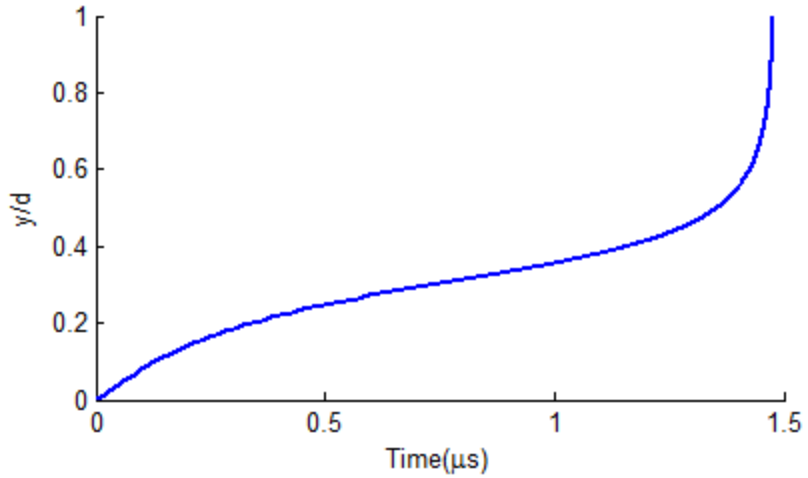

Figure 2.15: Pull-in-effect at an input voltage of 4 volts.

In analyzing the response of a MEMS, we may be able to determine the upper plate position due to an applied voltage. However it is important to analyze the transient behavior of the MEMS to be able to understand MEMS dynamics in particular if the MEMS is to be integrated with other components. Figure 2.16 shows the behavior of the MEMS with the parameters given above with different damping coefficient and a static voltage driving.

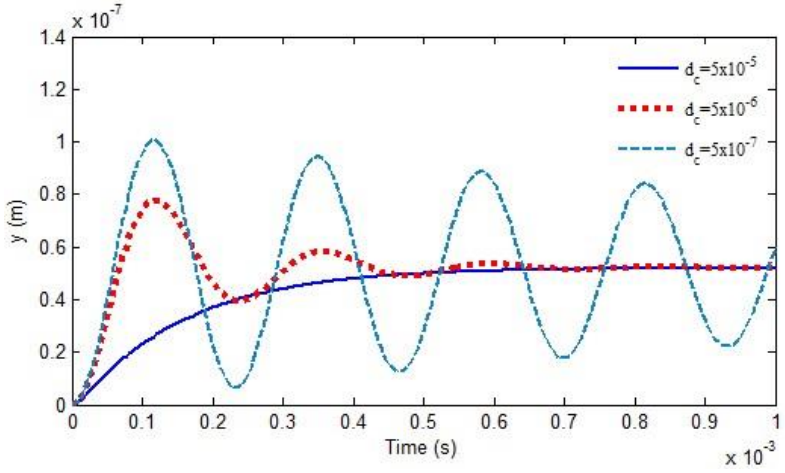

Figure 2.16: The transient response with different damping coefficient and a constant driving force.

For light damping, the upper plate will move passing the equilibrium position back and forth before it settles at the balanced position. The plate passes the balanced position reaches a maximum displacement y and returns passing the balanced position again. So, with light damping the plates oscillates before it settles at the equilibrium position. In that case, overshooting may occur if the applied driving force is close to the pull-in-voltage in which the two electrode will collapse, thus analysis will be carried out for the heavily damped case.

Chapter 3 presents an approximate analytical closed form solution to the non-linear differential equation (2.9) without the steady state assumption for impulse, step, ramp and sinusoidal as sources. The analytical results follow closely for small signal sources within 1% of the numerical results, thus allowing control of the plate's position and capacitive detection with reasonable accuracy.

Chapter3: Analysis of the Response of MEM Devices

3.1 Introduction

In this chapter we present an approximate closed form solution to the non-linear differential equation (2.9) for impulse, step and ramp. Also, we present a comparison of the analytical and numerical results (MATLAB). Later in this chapter we present a Simulink model for the memcapacitor.

3.2 Impulse Input Response and Analysis

Equation (2.9), listed below for convenience, describes the motion of the upper plate for a memcapacitor.

$$m\frac{d^2y(t)}{dt^2}+d_c\frac{dy(t)}{dt}+ky(t)=\frac{A\varepsilon_0 V_s^{\,2}}{2(d-y(t))^2}$$

where V_s is the source voltage. If $V_s=\delta(t)$, the Dirac-Delta function, then (2.9) becomes

$$m\frac{d^2y(t)}{dt^2}+d_c\frac{dy(t)}{dt}+ky(t)=\frac{A\varepsilon_0\ \delta(t)^{\,2}}{2(d-y(t))^2} \tag{3.1}$$

Applying Laplace transform to (3.1),

$$\mathcal{L}\left(m\frac{d^2y(t)}{dt^2}+d_c\frac{dy(t)}{dt}+ky(t)\right)=\ \mathcal{L}\ \left(\frac{A\varepsilon_0\ \delta(t)^{\,2}}{2(d-y(t))^2}\right) \tag{3.2}$$

with zero initial conditions, we get

$$Y(s)(ms^2+d_cs+k)=\mathcal{L}\ \left(\frac{A\varepsilon_0\ \delta(t)^{\,2}}{2(d-y(t))^2}\right) \tag{3.3}$$

$$Y(s) = \left(\frac{1}{(ms^2 + d_c s + k)} \right) \mathcal{L} \left(\frac{A\varepsilon_0 \ \delta(t)^{\ 2}}{2(d - y(t))^2} \right) \tag{3.4}$$

$$y(t) = \left(\frac{A\varepsilon_0 \ \delta(t)^{\ 2}}{2(d - y(t))^2} \right) * \left(\frac{\exp(-at)\sinh(c_1 t)}{mc_1} \right) \tag{3.5}$$

where $*$ denotes convolution and

$$\mathcal{L} \left(\frac{\exp(-at)\sinh(c_1 t)}{mc_1} \right) = \left(\frac{1}{(ms^2 + d_c s + k)} \right) \tag{3.6}$$

Where

$c_1 = \sqrt{\left(\frac{d_c}{2m} \right)^2 - \frac{k}{m}}$, $a = \frac{d_c}{2m}$ and $\left(\frac{d_c}{2m} \right)^2 > \frac{k}{m}$.

thus $$y(t) = \int_0^t \frac{A\varepsilon_0 \ \delta(t-\tau)^{\ 2}}{2 \ d - y(t-\tau)^{\ 2}} \frac{\exp\left(\frac{-d_c \tau}{2m} \right) \sinh(c_1 \tau)}{c_1 m} \, d\tau \tag{3.7}$$

with $y(0) = 0$

$$y(t) = \left(\frac{A\varepsilon_0}{2d^2 c_1 m} \right) \exp\left(-\frac{d_c}{2m} t \right) \sinh \ c_1 t \tag{3.8}$$

Equation (3.8) is the impulse response of the system. Figure 3.1 shows the plot of the impulse response for two different peaks.

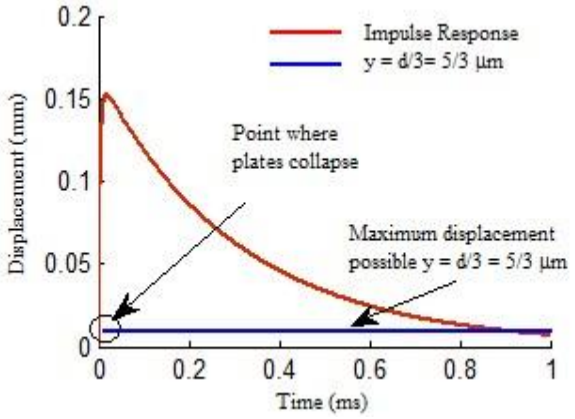

Figure 3.1: a) Impulse response with $V_s = \delta(t)$.

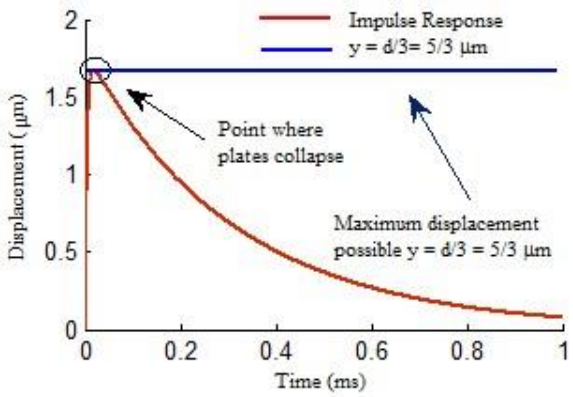

Figure 3.1: b) Impulse response with $V_s = 0.0033\delta(t)$.

As expected the upper plate travels a certain distance and is pulled back by the recovery force to the original position. The result in Figure 3 a) shows that there is overshooting caused by the electro-static-force due to the application of $V_s = \delta(t)$. That is, the system will overshoot if the voltage is ramped to its nominal value rapidly. Figure 3 b) shows that the system will not overshoot with $V_s = 0.0033\delta(t)$ V. To avoid overshooting caused by the electrostatic force, the voltage should ramp up to its nominal value slowly or the structure should be heavily damped [11].

3.3 Step Input Response and Analysis

The step input response is obtained by substituting $V_s = Bu(t)$ in (2.9).

$$m\frac{d^2y(t)}{dt^2} + d_c\frac{dy(t)}{dt} + ky(t) = \frac{A\varepsilon_0 V_s^{\,2}}{2\ d - y(t)^{\ 2}}$$

we get,

$$m\frac{d^2y(t)}{dt^2} + d_c\frac{dy(t)}{dt} + ky(t) = \frac{A\varepsilon_0 B^2}{2\ d - y(t)^{\ 2}} \tag{3.9}$$

$$m\frac{d^2y(t)}{dt^2} + d_c\frac{dy(t)}{dt} + ky(t) = \frac{A\varepsilon_0 B^2}{2d^2\left(1-\frac{y(t)}{d}\right)^2}$$

with $\frac{y(t)}{d} < 1$ for all t, we can write the geometric series expansion of the term to the right of (3.9) that is

$$\frac{A\varepsilon_0 B^2}{2\ d - y\ t^{\ 2}} = \frac{A\varepsilon_0 B^2}{2d^2\left(1-\frac{y}{d}\right)^2} = \frac{A\varepsilon_0 B^2}{2d^{\,2}}\left(\sum_{n=0}^{\infty}\left(\frac{y}{d}\right)^n\right)^2 \tag{3.10}$$

$$= \frac{A\varepsilon_0 B^2}{2d^{\,2}}\left(\sum_{n=0}^{\infty}\ n+1\left(\frac{y}{d}\right)^n\right)$$

$$= \frac{A\varepsilon_0 B^2}{2d^2}\left(1+\frac{2y}{d}+\frac{3y^2}{d^2}+\frac{4y^3}{d^3}+\text{.....}+\frac{(n+1)y^n}{d^n}\text{...}\right) \tag{3.11}$$

$$\left(\frac{3y^2}{d^2}+\frac{4y^3}{d^3}+.....+\frac{(n+1)y^n}{d^n}...\right)=\left(\frac{1}{\left(1-\frac{y(t)}{d}\right)^2}-1-\frac{2y(t)}{d}\right) \qquad (3.12)$$

For a step input, $y(t)$ is an increasing function of time, the minimum value of $y(t)$ is 0, and the maximum value is the steady state value. The steady state value is obtained by solving (2.9)

$$m\frac{d^2y(t)}{dt^2}+d_c\frac{dy(t)}{dt}+ky(t)=\frac{A\varepsilon_0 V_s^{\,2}}{2\ d-y(t)^{\ 2}}$$

under steady state conditions, that is solving:

$$ky(t)=\frac{A\varepsilon_0 V_s^{\,2}}{2(d-y(t))^2}$$

With $V_s=u(t)$, and parameters mentioned above and listed below for convenience:

$\varepsilon_0=8.854\,\text{x}10^{-12}$	F / m,	$d=5\,\text{x}10^{-6}$	m
$k=0.3125$	N / m,	$d_c=10^{-4}$	Kg / s
$m=2\,\text{x}10^{-6}$	Kg,	$A=9\,\text{x}10^{-8}$	m^2

Equation (2.10) yields three solutions $y_1=5.207\text{x}10^{-8}$ m, $y_2=4.465\text{x}10^{-6}$ m and

$y_3=0.000005482$ m. Solution $y_3>d$ is not a physical solution, and solution $y_2>\frac{d}{3}$ is not a stable solution, since for that value of *y* the two plates collapse, thus the only stable solution is

$y_1=0.00000005207$ m.

Thus $y_{\min} = 0$ and $y_{\max} = 5.207\text{x}10^{-8}$, substituting in (3.12) we get,

$$\left(\frac{1}{\left(1-\frac{y(t)}{d}\right)^2} - 1 - 2\frac{y(t)}{d} \right) = \begin{cases} 0 & \text{for} \quad y = 0 \\ 4.5613\text{x}10^{-6} & \text{for} \quad y = 5.207\,\text{x}10^{-8} \end{cases}$$

In either case the value obtained is too small compared with the values obtained for

$$\left(1+\frac{2y(t)}{d}\right) = \begin{cases} 1 & \text{for} \quad y = 0 \\ \\ 1.0208 & \text{for} \quad y = 5.207\,\text{x}10^{-8} \end{cases}$$

therefore,

$$\frac{A\varepsilon_0 B^2}{2d^2}\left(1+\frac{2y}{d}+\frac{3y^2}{d^2}+\frac{4y^3}{d^3}+.....+\frac{(n+1)y^n}{d^n}\right) \approx \frac{A\varepsilon_0 B^2}{2d^2}\left(1+\frac{2y}{d}\right)$$

thus (3.9) becomes

$$m\frac{d^2y(t)}{dt^2} + d_c\frac{dy(t)}{dt} + ky(t) \approx \frac{A\varepsilon_0 B^2}{2d^2}\left(1+\frac{2y(t)}{d}\right) \qquad (3.13)$$

Applying Laplace transform to (3.13),

$$Y(s)\ ms^2 + d_c s + k\ = \frac{A\varepsilon_0 B^2}{2d^2}\left(\frac{1}{s}+\frac{2Y(s)}{d}\right) \qquad (3.14)$$

$$Y(s) = \frac{\frac{A\varepsilon_0}{2d^2}B^2}{ms\left(s^2 + \frac{d_c}{m}s + \frac{k}{m} - \frac{A\varepsilon_0 B^2}{md^3}\right)}$$

$$= \frac{A\varepsilon_0 B^2}{2md^2}\left(\frac{p}{s} + \frac{qs + r}{\left(s + \frac{d_c}{2m}\right)^2 + \left(\frac{k}{m} - \frac{A\varepsilon_0 B^2}{md^3}\right) - \frac{d_c{}^2}{4m^2}}\right)$$

With $\left(\frac{k}{m} - \frac{A\varepsilon_0 B^2}{md^3}\right) - \frac{d_c{}^2}{4m^2} < 0$

Applying the inverse Laplace

$$y(t) = \frac{A\varepsilon_0 B^2}{2md^2}\left(p + q\exp\left(-\frac{d_c t}{2m}\right)\cosh\ c_2 t\ + \frac{r}{c_2}\exp\left(-\frac{d_c t}{2m}\right)\sinh\ c_2 \mathrm{t}\ \right) \qquad (3.15)$$

Where $c_2 = \sqrt{\frac{d_c{}^2}{4m^2} + \frac{A\varepsilon_0 B^2}{md^3} - \frac{k}{m}}$

With $y(0) = 0, y'(0) = 0$ and y''(0) = $\frac{A\varepsilon_0 B^2}{2md^2}$ we get,

$$q = \frac{1}{c_2{}^2 - a^2},\ p = \frac{1}{a^2 - c_2{}^2} \text{ and } r = \frac{a}{c_2{}^2 - a^2}$$

Thus $y(t) = \frac{A\varepsilon_0 B^2}{2md^2}\left(\frac{1}{a^2 - c_2{}^2} + \frac{1}{c_2{}^2 - a^2}\exp\left(-\frac{d_c t}{2m}\right)\cosh\ c_2 t + \frac{a}{c_2\ a^2 - c_2{}^2}\exp\left(-\frac{d_c t}{2m}\right)\sinh\ c_2 \mathrm{t}\right)$ (3.16)

Figures 3.2, 3.3, 3.4a and 3.4b show the numerical (MATLAB), analytical and both analytical and numerical plots. The percentage difference between the two analyses is 1.14×10^{-9} % for $V_s = u(t)$, 0.6% for $V_s = 2u(t)$, and 15.3% for $V_s = 3u(t)$.

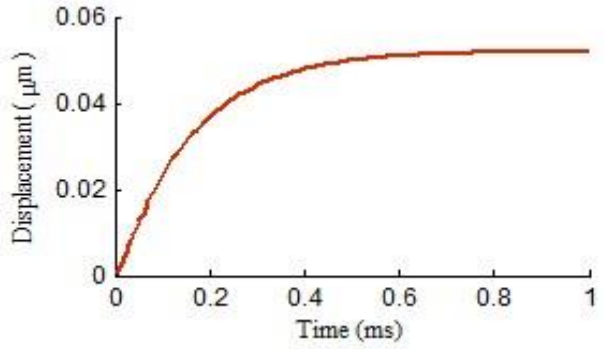

Figure 3.2: Numerical (MATLAB) solution with $V_s = u(t)$

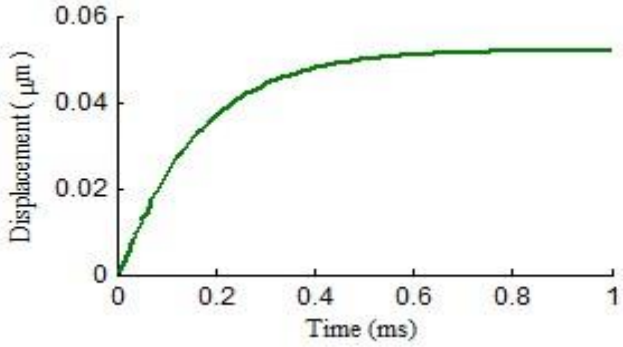

Figure 3.3: Analytical solution with $V_s = u(t)$

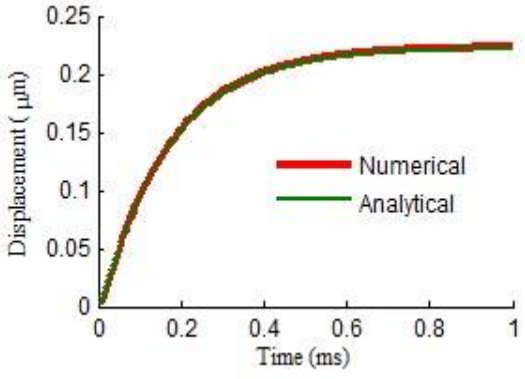

Figure 3.4: a) Numerical and Analytical $V_s = 2u(t)$

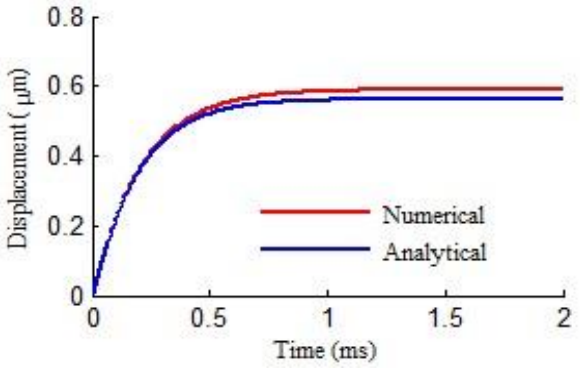

Figure 3.4: b) Numerical and Analytical solution $V_s = 3u(t)$

3.4 Ramp Input Response and Analysis

In the previous section, we discussed the response of a MEM to a step input. Since the steady state value was independent of time or pulse width, we found out that the position of the moving plate could be determined with a high degree of closeness to the numerical (MATLAB) value. In the case of a ramp input, $V_s(t) = t,$ the final position of the plate depends on the pulse width. Let $V_s(t) = t$, then (2.9) becomes

$$m\frac{d^2y(t)}{dt^2} + d_c\frac{dy(t)}{dt} + k\,y(t) = \frac{A\varepsilon_0 t^2}{2\ d - y(t)^{\ 2}} \tag{3.17}$$

With $\frac{y(t)}{d} < 1$ for all *t*,

$$\frac{A\varepsilon_0 t^2}{2\ d - y\ t^{\ 2}} = \frac{A\varepsilon_0 t^2}{2d^2\left(1-\frac{y}{d}\right)^2} = \frac{A\varepsilon_0 t^2}{2d^2}\left(\sum_{n=0}^{\infty}\left(\frac{y}{d}\right)^n\right)^2 = \frac{A\varepsilon_0 t^2}{2d^2}\left(\sum_{n=0}^{\infty}\ n+1\left(\frac{y}{d}\right)^n\right) \tag{3.18}$$

$$= \frac{A\varepsilon_0 t^2}{2d^2}\left(1+\frac{2y}{d}+\frac{3y^2}{d^2}+\frac{4y^3}{d^3}+.....+\frac{(n+1)y^n}{d^n}\right) \tag{3.19}$$

$$\left(\frac{2y}{d}+\frac{3y^2}{d^2}+\frac{4y^3}{d^3}+.....+\frac{(n+1)y^n}{d^n}\right) = \left(\frac{1}{\left(1-\frac{y(t)}{d}\right)^2}-1\right) \tag{3.20}$$

The value of (3.20) depends on the displacement $y(t)$. The maximum value $y(t)$ may have is $\frac{d}{3}$, which is the value obtained when the source voltage is equal to the pull-in voltage.

From (2.16) the pull-in voltage is:

$$V_s = \sqrt{\frac{8kd^3}{27A\varepsilon_0}}$$

with $V_s(t) = t$, and

$\varepsilon_0 = 8.854 \text{x} 10^{-12}$	F / m
$d = 5 \text{x} 10^{-6}$	m
$k = 0.3125$	N / m
$d_c = 5 \text{x} 10^{-5}$	Kg / s
$m = 2 \text{x} 10^{-6}$	Kg
$A = 9 \text{x} 10^{-8}$	m^2

We get $t = 3.811$ seconds, that means the pulse width of the ramp should be less than 3.811 seconds in order for the plates not to collapse (see Figure 3.5).

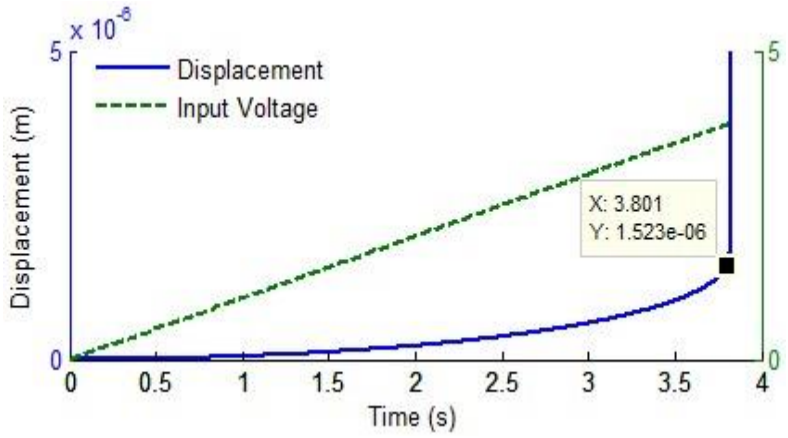

Figure 3.5: Numerical solution of the displacement y with ramp input $V_s(t) = t$.

If $y(t) << d$, then (3.17) reduces to

$$m\frac{d^2y(t)}{dt^2} + d_c\frac{dy(t)}{dt} + k\,y(t) = \frac{A\varepsilon_0 t^2}{2d^2} \qquad (3.21)$$

The solution to (3.21) with $y'(0) = 0$, and $y''(0) = 0$ is,

$$y(t)=\frac{A\varepsilon_0}{2mc_1d^2}\left\{\begin{array}{l}\dfrac{\exp\ c_1-a\ t}{c_1-a^{\ 3}}+\dfrac{\exp\ -c_1+a\ t}{(c_1+a)^3}+\left(\dfrac{-1}{2\ c_1-a}+\dfrac{-1}{(2(c_1+a))}\right)t^2\\ +\left(\dfrac{1}{c_1-a^{\ 2}}-\dfrac{1}{c_1+a^{\ 2}}\right)t-\dfrac{1}{c_1-a^{\ 3}}-\dfrac{1}{c_1+a^{\ 3}}\end{array}\right\} \quad (3.22)$$

where $c_1=\left(\frac{d_c^{\ 2}}{4m^2}-\frac{k}{m}\right)^{0.5}$.

Figure 3.6 shows the numerical solution (MATLAB) for (3.17) and the solution for (3.21).

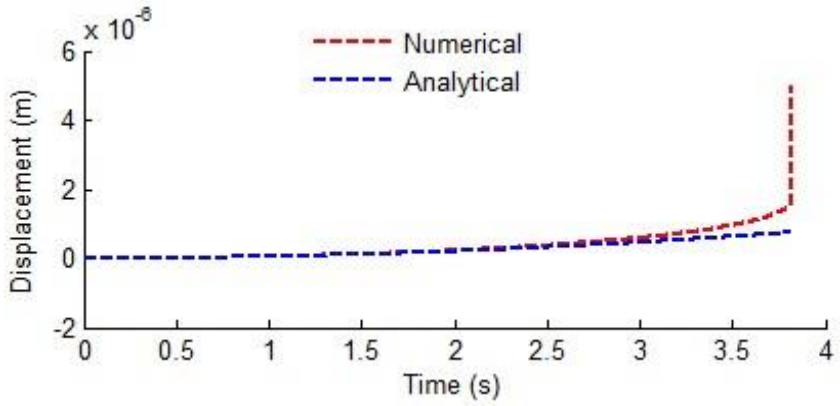

Figure 3.6: Numerical and analytical solution of the displacement y
with ramp input $V_s(t)=t$.

Also, it shows that if the pulse width is smaller than the pull-in-effect time (time when the plates collapse), then an approximate equation of the displacement $y(t)$ can be obtained with minimal error.

Suppose the pulse width of the input ramp is 2 seconds, since $y(t)$ is an increasing function of time, then the maximum value that $y(t)$ can reach is when it reaches its final position. At that point we have $y'(t)=y''(t)=0$ and $t=2$. Substituting $y'(t)=y''(t)=0$ and $t=2$ in (3.21) we get,

$$ky(t) = \frac{4A\varepsilon_0}{2(d - y(t))^2} \tag{3.23}$$

There are three solution to (3.23).

$$y_1 = 5.67\text{x}10^{-6},\ y_2 = 1.0649\,\text{x}10^{-7},\ \text{and}\ \ y_3 = 4.229\,\text{x}10^{-6}$$

The first solution, has no physical meaning since $y_1 > d$. The third solution $y_3 > \frac{d}{3}$, and thus unstable. The only valid solution is $y_2 = 1.0649\,\text{x}10^{-7}$.

With $y = 1.0649\,\text{x}10^{-7}$ the right hand side of (3.20) becomes

$$\left\{\frac{1}{\left(1-\frac{y(t)}{d}\right)^2} - 1\right\} = \left\{\frac{1}{\left(1-\frac{1.0649\ \text{x}\ 10^{-7}}{5\ \text{x}\ 10^{-6}}\right)^2} - 1\right\} = 0.0208 << 1$$

Thus, with a ramp input with a pulse width t =2, (2.9) can be approximated by (3.21), hence

$$m\frac{d^2y(t)}{dt^2} + d_c\frac{dy(t)}{dt} + ky(t) = \frac{A\varepsilon_0\ t^2}{2\ \left(d - y(t)\right)^2}$$

$$\approx m\frac{d^2y(t)}{dt^2} + d_c\frac{d\,y(t)}{dt} + k\,y(t) = \frac{A\varepsilon_0\,t^2}{2d^2}$$

Figure 3.7 shows both analytical and numerical (MATLAB) solutions.

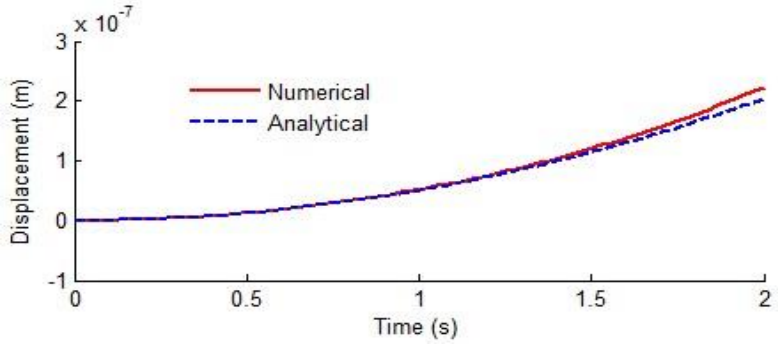

Figure 3.7: Numerical and analytical solution of the displacement y with ramp input $V_s(t) = t$ of a pulse width 2 seconds.

The maximum difference is

$$\varepsilon_{\max} = \frac{y(actual) - y(analytical)}{y(actual)} \text{x}100\% = \frac{2.23\text{x}10^{-7} - 2.039\text{x}10^{-7}}{2.23\text{x}10^{-7}} \text{x}100\% \sim 8\%$$

Repeating the above with a ramp input with pulse width of 1 seconds, then the maximum value that $y(t)$ can reach is found by solving (2.10),

$$ky(t) = \frac{A\varepsilon_0 t^2}{2(d - y(t))^2},$$

with $t = 1$. The only valid solution is $y = 5.20\text{x}10^{-8}$. Then the right hand side of

$$\left(\frac{2y}{d} + \frac{3y^2}{d^2} + \frac{4y^3}{d^3} + ... + \frac{n+1\ y^n}{d^n} \right) = \left(\frac{1}{\left(1 - \frac{y(t)}{d}\right)^2} - 1 \right)$$

reduces to

$$\left(\frac{1}{\left(1 - \frac{y(t)}{d}\right)^2} - 1 \right) = \left(\frac{1}{\left(1 - \frac{5.2\text{x}10^{-8}}{5\text{x}10^{-6}}\right)^2} - 1 \right) = 0.0021 << 1$$

Thus with a ramp input with a pulse width $t = 1$, (2.9) can be approximated by (3.21), hence

$$m\frac{d^2y(t)}{dt^2} + d_c\frac{dy(t)}{dt} + ky(t) = \frac{A\varepsilon_0 t^2}{2\ d - y(t)^2}$$

$$\approx m\frac{d^2y(t)}{dt^2} + d_c\frac{d\,y(t)}{dt} + k\,y(t) = \frac{A\varepsilon_0 t^2}{2d^2}$$

Figure 3.8 shows both analytical and numerical (MATLAB) solutions.

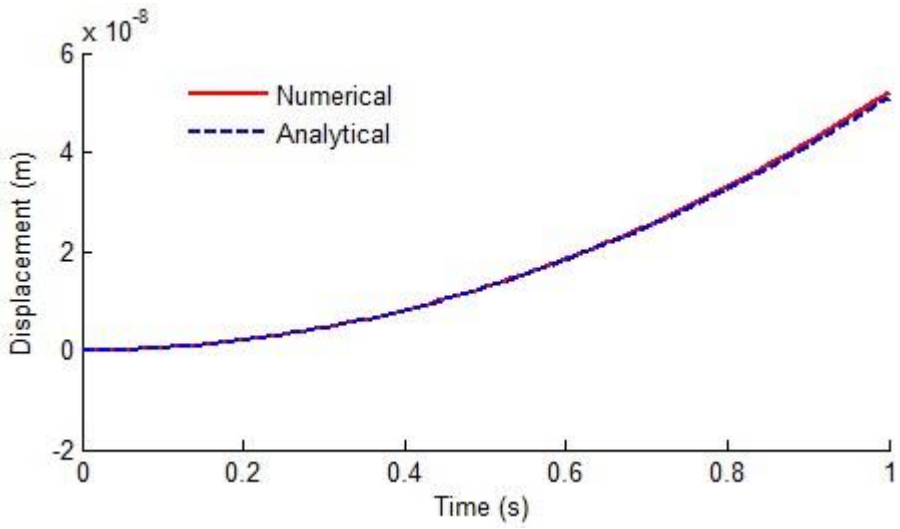

Figure 3.8: Numerical and analytical solution of the displacement *y* with ramp input $V_s(t) = t$ of a pulse width 1 seconds.

The maximum difference is

$$\varepsilon_{\max} = \frac{y(actual) - y(analytical)}{y(actual)} \text{x} 100\% = \frac{5.20 \text{x} 10^{-8} - 5.09 \text{x} 10^{-8}}{5.20 \text{x} 10^{-8}} \text{x} 100\% \sim 2\%$$

A similar analysis is done for a ramp with pulse width of 0.5 seconds. Figures 3.9 and 3.10 show the numerical (MATLAB) and analytical solutions for the displacement of the upper plate.

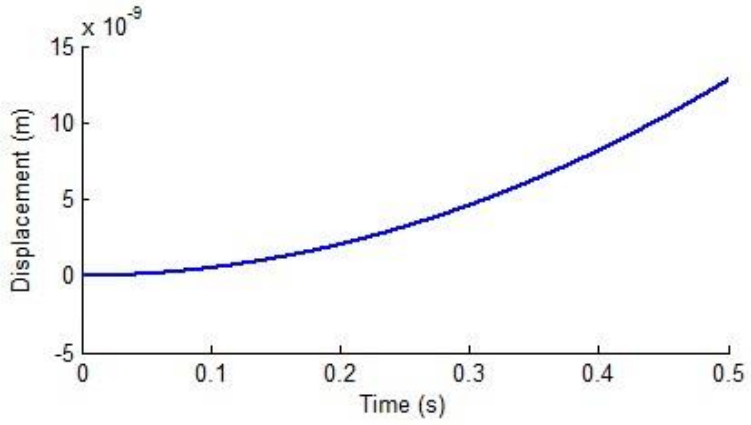

Figure 3.9: Numerical solution of the displacement y (t) with input $V_s(t) = t$ with pulse width of 0.5 seconds.

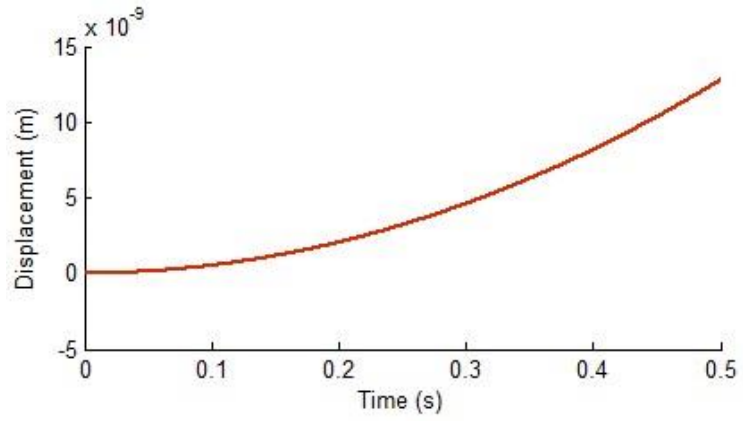

Figure 3.10: Analytical solution of the displacement y(t) with input $V_s(t) = t$ with pulse width of 0.5 seconds.

The maximum difference is

$$\varepsilon_{\max} = \frac{y(actual) - y(analytical)}{y(actual)} \text{x}100\% = \frac{4.9392\,\text{x}10^{-12} - 4.9392\,\text{x}10^{-12}}{4.9392\,\text{x}10^{-12}} \text{x}100\% = 0\%$$

3.5 Sinusoidal Input Response and Analysis

In the previous section, we discussed the response of a MEM to a ramp input. Since the steady state value was dependent on time or pulse width, we found out that the position of the moving plate could be determined with a high degree of closeness to the numerical (MATLAB) value if the pulse width is small. In the case of a sinusoidal input, $V_s(t) = V_m \sin(wt),$ the displacement of the upper electrode reaches a steady state sinusoidal form with an amplitude depending on the amplitude and frequency of the input.

Let $V_s(t) = V_m \sin(wt),$ then (2.9) becomes

$$m\frac{d^2y(t)}{dt^2} + d_c\frac{dy(t)}{dt} + k\,y(t) = \frac{A\varepsilon_0 {V_m}^2 \sin^2(wt)}{2\left(d - y(t)\right)^2} \tag{3.24}$$

Applying Laplace transform to (3.24), with $y'(0) = 0$, and $y''(0) = 0$,

$$\mathcal{L}\left(m\frac{d^2y(t)}{dt^2} + d_c\frac{dy(t)}{dt} + ky(t)\right) = \mathcal{L}\left(\frac{A\varepsilon_0 {V_m}^2 \sin^2(wt)}{2\ d - y(t)^{\ 2}}\right) \tag{3.25}$$

or

$$Y(s)(ms^2 + d_c s + k) = \mathcal{L}\left(\frac{A\varepsilon_0 {V_m}^2 \sin^2(wt)}{2\ d - y(t)^{\ 2}}\right) \tag{3.26}$$

$$Y(s) = \left(\frac{1}{(ms^2 + d_c s + k)}\right)\ \mathcal{L}\left(\frac{A\varepsilon_0 {V_m}^2 \sin^2(wt)}{2\ d - y(t)^{\ 2}}\right) \tag{3.27}$$

$$y(t) = \left(\frac{A\varepsilon_0 V_m{}^2 \sin^2(wt)}{2\ d - y(t)^{\ 2}} \right) * \left(\frac{\exp(-at)\sinh(c_1 t)}{mc_1} \right) \tag{3.28}$$

where $*$ denotes convolution and

$$\mathcal{L}\ \left(\frac{\exp(-at)\sinh(c_1 t)}{mc_1} \right) = \left(\frac{1}{(ms^2 + d_c s + k)} \right) \tag{3.29}$$

where

$$c_1 = \sqrt{\left(\frac{d_c}{2m} \right)^2 - \frac{k}{m}},\ a = \frac{d_c}{2m} \quad \text{and} \quad \left(\frac{d_c}{2m} \right)^2 > \frac{k}{m}.$$

thus

$$y(t) = \int_0^t \frac{A\varepsilon_0 V_m{}^2 \sin^2\ w(t-\tau)}{2\ d - y(t-\tau)^{\ 2}} \frac{\exp\left(\frac{-d_c \tau}{2m} \right)\sinh(c_1 \tau)}{c_1 m}\ d\tau \tag{3.30}$$

Since

$$0 \le \sin^2\ w(t-\tau)\ \le 1,$$

and

$$\frac{1}{2\left(d - y(t-\tau)\right)^2} \le \frac{9}{8d^2} \qquad \text{for } y \le \frac{d}{3},$$

then

$$y(t) \le \frac{9A\varepsilon_0 V_m{}^2}{8d^2 c_1 m} \int_0^t \exp\left(\frac{-d_c \tau}{2m} \right)\sinh(c_1 \tau)\ d\tau \tag{3.31}$$

$$y(t) \le \frac{9A\varepsilon_0 V_m{}^2}{16d^2 c_1 m}\int_0^t \left(\exp\left(c_1 - \frac{d_c}{2m}\right)\tau - \exp\left(-c_1 - \frac{d_c}{2m}\right)\tau\right)d\tau$$

$$y(t) \le \frac{9A\varepsilon_0 V_m{}^2}{16d^2 c_1 m}\left(\frac{\exp\left(c_1 - \frac{d_c}{2m}\right)\tau}{\left(c_1 - \frac{d_c}{2m}\right)} + \frac{\exp\left(-c_1 - \frac{d_c}{2m}\right)\tau}{\left(c_1 + \frac{d_c}{2m}\right)}\right)_0^t$$

$$y(t) \le \frac{9A\varepsilon_0 V_m{}^2}{16d^2 c_1 m}\left(\frac{\exp\left(c_1 - \frac{d_c}{2m}\right)t}{\left(c_1 - \frac{d_c}{2m}\right)} + \frac{\exp\left(-c_1 - \frac{d_c}{2m}\right)t}{\left(c_1 + \frac{d_c}{2m}\right)}\right) + \frac{9A\varepsilon_0 V_m{}^2}{8d^2 k}$$

where $c_1 = \sqrt{\left(\frac{d_c}{2m}\right)^2 - \frac{k}{m}}$,

With the parameters of the MEMS,

$\varepsilon_0 = 8.854\,\text{x}10^{-12}$	F / m
$d = 5\,\text{x}10^{-6}$	m
$k = 0.3125$	N / m
$d_c = 5\,\text{x}10^{-5}$	Kg / s
$m = 2\,\text{x}10^{-6}$	Kg
$A = 9\,\text{x}10^{-8}$	m^2

then $\left(c_1 - \frac{d_c}{2m}\right) < 0$, and the maximum value of the displacement $y(t)$ is

$$\frac{9A\varepsilon_0 {V_m}^2}{16d^2 c_1 m}\left(\frac{\exp\left(c_1-\frac{d_c}{2m}\right)t}{\left(c_1-\frac{d_c}{2m}\right)}+\frac{\exp\left(-c_1-\frac{d_c}{2m}\right)t}{\left(c_1+\frac{d_c}{2m}\right)}\right)+\frac{9A\varepsilon_0 {V_m}^2}{8d^2k}=\frac{9A\varepsilon_0 {V_m}^2}{8d^2k}$$

$\lim\ t \to \infty$

Therefore

$$y_{\max}=\frac{9A\varepsilon_0 {V_m}^2}{8d^2k} \tag{3.32}$$

Since $y_{\max} \le \frac{d}{3}$, then solving (3.32) for V_m we get,

$$V_m \le \sqrt{\frac{8kd^3}{27A\varepsilon_0}}$$

For $V_m = 1$, that is a source voltage $V_s = \sin(wt)$, (3.17) becomes

$$m\frac{d^2y(t)}{dt^2}+d_c\frac{dy(t)}{dt}+k\,y(t)=\frac{A\varepsilon_0\sin^2(wt)}{2\ d-y(t)^{\ 2}} \tag{3.33}$$

Expanding the right hand side of (3.33) as a geometric series,

$$\frac{A\varepsilon_0\sin^2(wt)}{2\ d-y\ t^{\ 2}}=\frac{A\varepsilon_0\sin^2(wt)}{2d^2\left(1-\frac{y}{d}\right)^2}=\frac{A\varepsilon_0\sin^2(wt)}{2d^2}\left(\sum_{n=0}^{\infty}\left(\frac{y}{d}\right)^n\right)^2$$

$$=\frac{A\varepsilon_0\sin^2(wt)}{2d^2}\left(\sum_{n=0}^{\infty}\ n+1\left(\frac{y}{d}\right)^n\right) \tag{3.34}$$

$$=\frac{A\varepsilon_0\sin^2(wt)}{2d^2}\left(1+\frac{2y}{d}+\frac{3y^2}{d^2}+\frac{4y^3}{d^3}+.....+\frac{(n+1)y^n}{d^n}...\right) \tag{3.35}$$

$$\left(\frac{2y}{d}+\frac{3y^2}{d^2}+\frac{4y^3}{d^3}+.....+\frac{n+1\ y^n}{d^n}...\right)=\left(\frac{1}{\left(1-\frac{y(t)}{d}\right)^2}-1\right) \tag{3.36}$$

Then $y_{\max}=\frac{9A\varepsilon_0}{8d^2k}=1.1475\text{x}10^{-7}$ we get,

$$\left(\frac{1}{\left(1-\frac{y(t)}{d}\right)^2}-1\right)=\left(\frac{1}{\left(1-\frac{1.1475\text{x}10^{-7}}{5\text{x}10^{-6}}\right)^2}-1\right)\approx 0.0234$$

Since $0.0234<<1$, then (3.33) reduces to

$$m\frac{d^2y(t)}{dt^2}+d_c\frac{dy(t)}{dt}+k\,y(t)\approx\frac{A\varepsilon_0\sin^2(wt)}{2d^2} \tag{3.37}$$

or
$$m\frac{d^2y(t)}{dt^2}+d_c\frac{dy(t)}{dt}+k\,y(t)\approx\frac{A\varepsilon_0\ 1-\cos(2wt)}{4d^2} \tag{3.38}$$

The solution to (3.38) is

$$y(t)=M\exp\ -a+c_1\ +N\exp\ -a-c_1\ +A_1\cos(2wt)+B_1\sin(2wt)+C_1 \tag{3.39}$$

Where M, N, A_1, B_1 and C_1 are constants, and

$$y_c(t)=M\exp\left(\frac{-d_c}{2m}+\sqrt{\frac{d_c^{\ 2}}{4m}-\frac{k}{m}}\right)+N\exp\left(\frac{-d_c}{2m}-\sqrt{\frac{d_c^{\ 2}}{4m}-\frac{k}{m}}\right) \tag{3.40}$$

$$y_p(t)=A_1\cos(2wt)+B_1\sin(2wt)+C_1 \tag{3.41}$$

are the complimentary and particular solutions respectively.

Substituting $\frac{d^2y_p(t)}{dt^2}, \frac{dy_p(t)}{dt}$ and $y_p(t)$ in (3.38) we get,

$$B_1 = \frac{-A\varepsilon_0 w d_c}{2d^2\ \ k\ -\ 4mw^2\ ^2 + 4w^2 d_c^{\ 2}},\ A_1 = \frac{-A\varepsilon_0 - 8wd_c B_1}{4d^2\ \ k - 4mw^2} \text{ and } C_1 = \frac{A\varepsilon_0}{4d^2 k}.$$

Substituting $\frac{d^2y_c(t)}{dt^2}, \frac{dy_c(t)}{dt}$ and $y_c(t)$ in (3.38) we get,

$$M = \frac{-\left(C_1\left(\frac{-d_c}{2m} + \sqrt{\frac{d_c^{\ 2}}{4m} - \frac{k}{m}}\right) + A_1\left(\frac{-d_c}{2m} + \sqrt{\frac{d_c^{\ 2}}{4m} - \frac{k}{m}}\right)k + 2wB_1 k\right)}{\left(2k\sqrt{\frac{d_c^{\ 2}}{4m} - \frac{k}{m}}\right)}$$

and

$$N = -\ C_1 + A_1 + M$$

where

$y(t)$ is the displacement of the plate
t is time
A is the area of the plate
d is the separation between the plates
ε_0 is the permittivity of free space
w is the angular frequency of the input signal

Figures 3.11 and 3.12 show the displacement *y* (*t*) for an input signal $V_s(t) = \sin(8000\pi t)$.

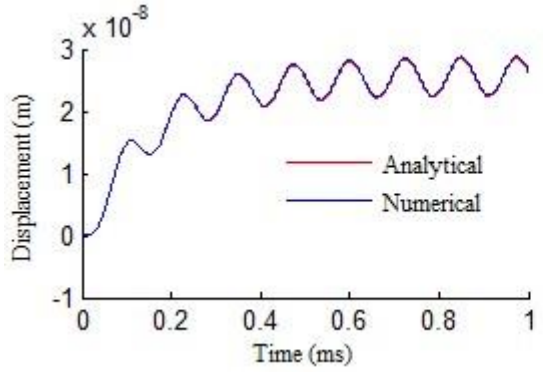

Figure 3.11: Numerical and Analytical solutions with input $V_s(t) = \sin(8000\pi t)$.

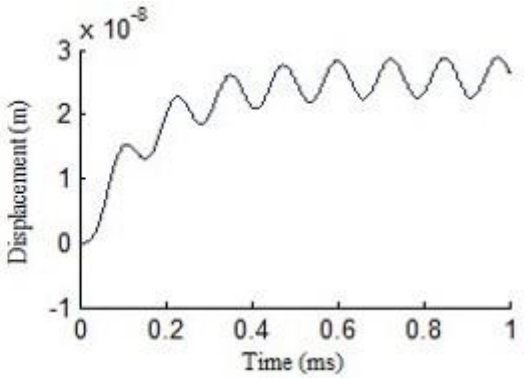

Figure 3.12: Numerical solution with input $V_s(t) = \sin(8000\pi t)$.

$$|\varepsilon_{\max}| = \left|\frac{y(actual) - y(analytical)}{y(actual)}\right| x100\% = \left|\frac{2.8539\,x10^{-8} - 2.8539\,x10^{-8}}{2.8539\,x10^{-8}}\right| x100\% \approx 0\%$$

Figure 3.13 shows the numerical and analytical results displacement *y* (*t*) for an input signal $V_s(t) = \sin(8\pi t)$.

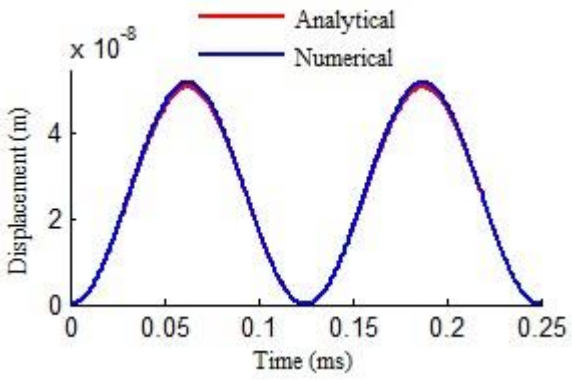

Figure 3.13: Numerical and Analytical solutions of the displacement y (*t*) with input $V_s(t) = \sin(8\pi t)$.

$$\left|\varepsilon_{\max}\right| = \left|\frac{y(actual) - \mathrm{y}(analytical)}{y(actual)}\right| \mathrm{x}100\% = \left|\frac{5.0998\,\mathrm{x}10^{-8} - \ 5.2082\,\mathrm{x}10^{-8}}{5.0998\,\mathrm{x}10^{-8}}\right| \mathrm{x}100\% \ \approx \ 2.1\%$$

Figure 3.14 shows the numerical and analytical solution for an input signal $V_s(t) = 2\sin(8000\pi t)$. Analysis shows an increase in percentage difference.

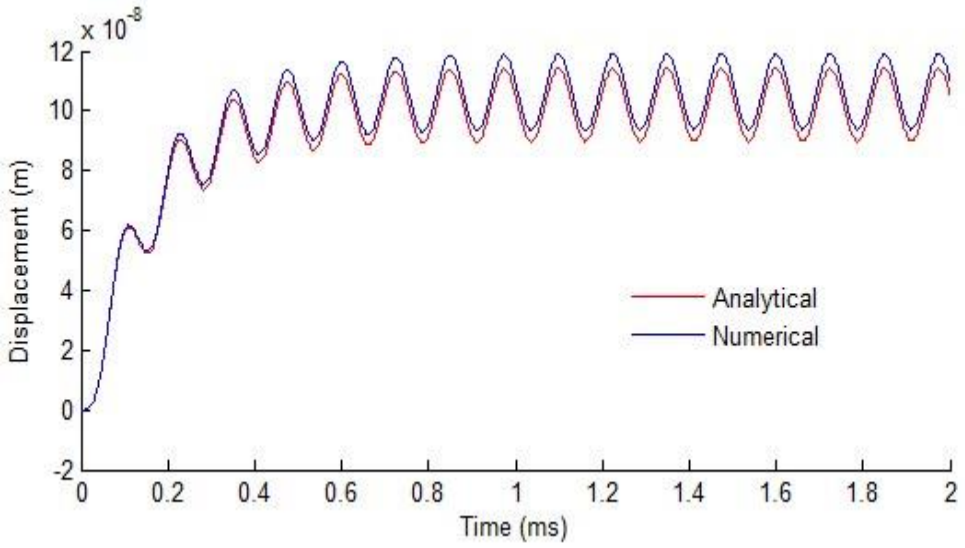

Figure 3.14: Numerical and Analytical solutions of the displacement y(t) with input $V_s(t) = 2\sin(8000\pi t)$.

$$\left|\varepsilon_{\max}\right| = \left|\frac{y(actual) - \mathrm{y}(analytical)}{y(actual)}\right| \mathrm{x}100\% = \left|\frac{1.1907\mathrm{x}10^{-7} - \ 1.1414\,\mathrm{x}10^{-7}}{1.1907\,\mathrm{x}10^{-7}}\right| \mathrm{x}100\% \ \approx \ 4.1\%$$

Figure 3.15 shows the numerical and analytical solution for an input signal with amplitude 2 and a frequency 4 Hz, $V_s(t) = 2\sin(8\pi t)$.

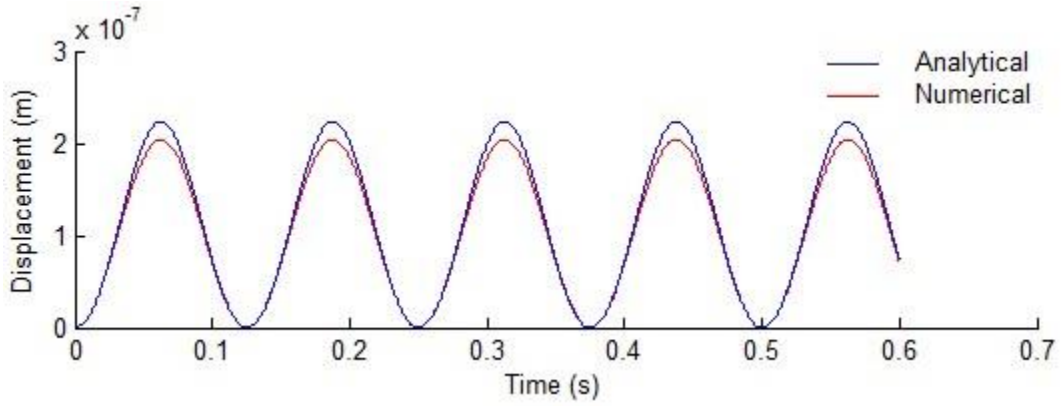

Figure 3.15: Numerical and Analytical solutions of the displacement y (t) with input $V_s(t) = 2\text{in}(8\pi t)$.

$|\varepsilon_{\max}| \approx 8\%$

Figures 3.16 and 3.17show the numerical and analytical solution for an input signal with amplitude 3 and frequencies 4 KHz and 4 Hz respectively.

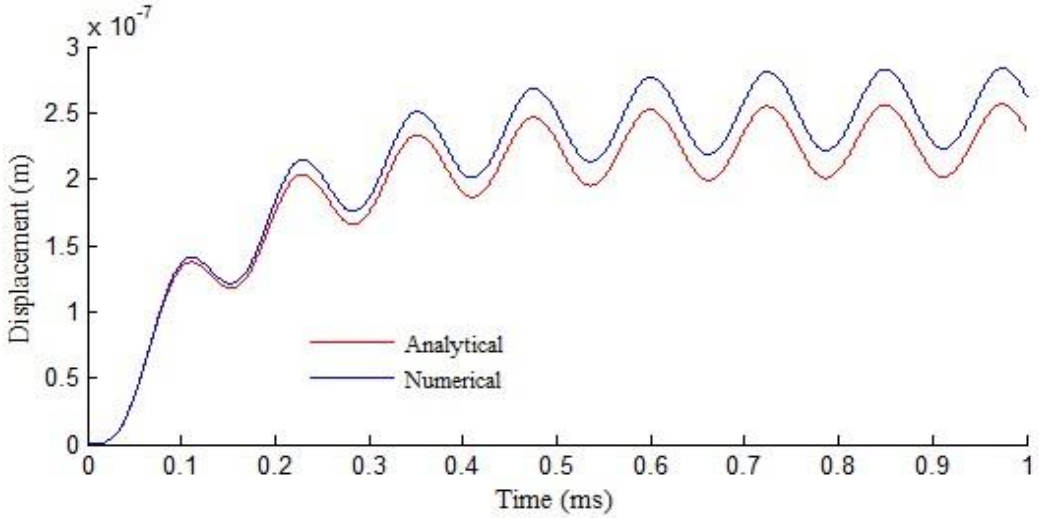

Figure 3.16: Numerical and Analytical solutions of the displacement y (t) with input $V_s(t) = 3\sin(8000\pi t)$.

$|\varepsilon_{\max}| \approx 9\%$.

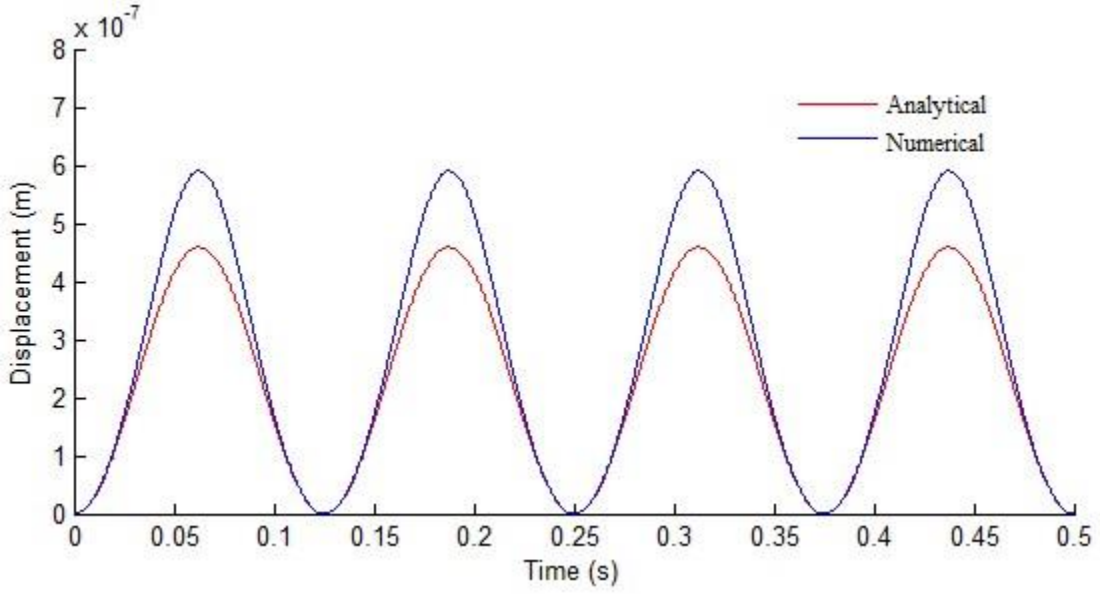

Figure 3.17: Numerical and Analytical solutions of the displacement y (t) with input $V_s(t) = 3\sin(8\pi t)$.

$|\varepsilon_{\max}| \approx 22.2\%$.

3.6 Simulink Model

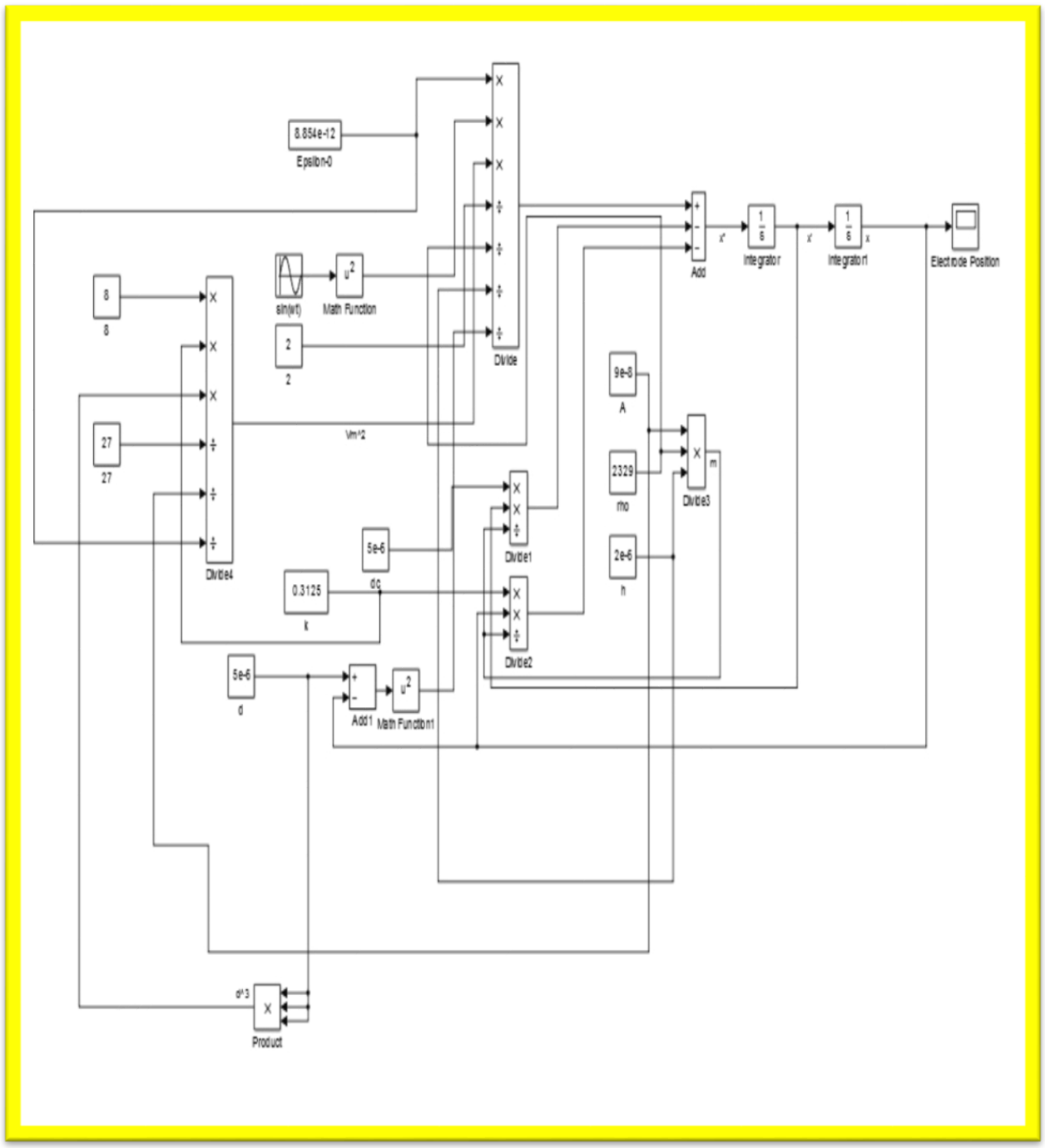

Figure 3.18: Simulink model with a sinusoidal input.

Chapter 4: Conclusion

MEMS can help in the miniaturization of various types of electronic products and devices. A MEMS can be as small as one cubic mm. Such a size helped in the miniaturization of mobile phones, computers and various types of electronic devices. Also, their small size tends to result in less power requirement and consumption, high volume production that cuts down the MEMS cost, and since MEMS are very reliable, as a result MEMS has become a revolutionary device.

This dissertation covers the finding of an approximate closed-form solution for the equation of the motion of the displacement of the upper plate of a MEMS by linearizing the non-linear electrostatic force in the differential equation describing the motion. The linearization was made by expanding the nonlinear term into a geometric series in the displacement, approximating it with the first two terms and showing that the remainder of the is small. The analysis was carried out for different input biasing such as impulse, step, ramp and sinusoidal. A comparison between the analytical and numerical solutions was made to calculate the error obtained for such approximation. Results show that for an input of almost 75% of the pull-in-voltage, the difference between the numerical and analytical values was less than 9% except for the case where the input was a sinusoidal with a frequency 4 Hz where the maximum difference was 22.2 %. For a low frequency input such as 4 Hz, the frequency of the electrostatic driving force is 8 Hz
which is much smaller than

$$f_{MEMS} = \frac{1}{2\pi}\sqrt{\frac{k}{m}} = 4.3453 \text{ kHz}$$

the natural frequency of the MEMS. That is the plate will travel a bigger distance than the case for higher frequencies. With large displacements y at low frequencies, the approximation of the

geometric series in y with the first two terms will yield larger errors as is in figure 3.17.

In all cases, the difference between the analytical and numerical transient parts of the response was less than 1%.

References

[1] Website http: //www.utexas.edu/news/engineers-build-fastest-nanomotor/(Accessed: 05 September 2014).

[2] History of MEMS, *Southwest Center for Microsystem Education,* [online] 2013, www.scmenm.org (Accessed: 21 January 2014).

[3] Patrick b. Chu, Phyllis R. Nelson, Mark L. Tachiki, Kristofer S. J. Pister, "Dynamics of Polysilicon parallel-plate electrostatic actuators", *Sensors and Actuators,* pp. 216-220.

[4] Web site, http://www.ryerson.ca/ (Accessed: 21 January 2014).

[5] Product design and development, emerging mems: technologies & markets, 2013 report.

[6] Allan R. Hambley, *Electrical Engineering Principles and Application, second edition,* Prentice Hall. (2002).

[7] Web site, http://www.electronics-tutorials.ws/capacitor/cap_4.html (Accessed: 21 January 2014).

[8] Web site, http://www.johnhearfield.com/Physics/Capacitance.htm (Accessed: 21January 2014).

[9] Ki Bang Lee, "Theoretical Dynamic Response of an Electrostatic Parallel Plate". *American Institute of Physics,* vol. 91, issue 18, 2007.

[10] R. Y. Vinokur, "Feasible Analytical Solution for Electrostatic Parallel–Plate Actuator or Sensor," *Journal of Vibration and Control,* vol.10, no.3, pp. 359-369, 2004.

[11] Minhang Bao, *Analysis and Design Principles of MEMS devices*, Elsevier. (2005).

[12] Martin H. Sadd, "*Elasticity: Theory, Application, and Numerics*", Academic Press. (2004).

[13] Seyed Kamaleddin, "*Nonlinear Systems Stability Analysis",* CRC Press. (2013).

APPENDIX

********** MEMS PARAMETERS **********

$e_0 = 8.854 \times 10^{-12}$	Vacuum permittivity	(F/m)
$d = 5 \times 10^{-6}$	Plates separation	(m)
$k = 0.3125$	Spring constant	(N/m)
$dc = 5 \times 10^{-5}$	Damping constant	(Kg/s)
Rho = 2329	Upper density plate	(Kg/ m^3)
$A = 9 \times 10^{-8}$	Plate area	(m^2)
$h = 2 \times 10^{-6}$	Upper plate thickness	(m)
m = rho x *A* x *h*	Upper electrode mass	(Kg)

MATLAB Program

```
function        ysol=Mems (t , y)
w=8*π;
vm=(8*k*d^3/(27*A*e0))^0.5;
C=A*e0*vm^2/(2*d^2)
ysol1=y(2);
ysol2=A*e0*(vm)^2*sin(w*t) / (2*m*(d-y(1))^2)-dc*y(2) / m-k*y(1)/m;
ysol=[ysol1;ysol2]
% options=odeset('RelTol',1e-7,'AbsTol',1e-7,'MaxStep',1e-2)
% [t, y]=ode23s(@Mems, [0 1], [0 0], options);
```

Curriculum Vitae

Ghassan Khalil Kachmar was born in Beirut, Lebanon. In 1979 he joined the University of Louisiana at Lafayette to pursue a Bachelor of Science in Electrical and Computer Engineering. After graduation in 1983, Dr. Kachmar moved to Limassol, Cyprus where he taught mathematics and electronics at the Green Hill Technical College.

In 1985, Dr. Kachmar joined the University of Texas at El Paso to pursue a Bachelor of Science in Mathematics. In 1987, he joined the El Paso Community College Math and Science department where he taught Math classes ranging from Basic Algebra to Differential Equations. In 1995, he joined New Mexica State University and in 1997 he received his Master of Science degree in Electrical Engineering (Communication Option). Through the years 1997 – 2012, Dr. Kachmar taught Mathematics at UTEP, EPCC and worked as Engineer for Powell Electric in Houston, Texas. In 2012 he joined the Doctoral Program in Electrical Engineering at The University of Texas at El Paso.

Dr. Kachmar authored the publication *"Modeling the Response of a Memcapacitor for Impulse, Step, Ramp, and Sinusoidal Inputs"*, and co-authored the publication of "*Analysis of the memristors and MEMS integration in a series circuit configuration"*

Permanent Address: Ghassan K. Kachmar,
5849 Sixta Dr.
El Paso, TX. 79932
U.S.A